FISEVIER

Contents lists available at ScienceDirect

Journal of Nuclear Materials

journal homepage: www.elsevier.com/locate/jnucmat



Effects of neutron irradiation on microstructures and hardness of stainless steel weld-overlay cladding of nuclear reactor pressure vessels



T. Takeuchi ^a,*, Y. Kakubo ^b, Y. Matsukawa ^b, Y. Nozawa ^b, T. Toyama ^b, Y. Nagai ^b, Y. Nishiyama ^c, J. Katsuyama ^c, Y. Yamaguchi ^c, K. Onizawa ^c

- ^a Oarai Research and Development Center, Japan Atomic Energy Agency, Oarai, Ibaraki 311-1393, Japan
- ^b The Oarai Center, Institute for Materials Research, Tohoku University, Oarai, Ibaraki 311-1313, Japan
- ^cNuclear Safety Research Center, Japan Atomic Energy Agency, Tokai, Ibaraki 319-1195, Japan

ARTICLE INFO

Article history: Available online 3 February 2014

ABSTRACT

The microstructures and the hardness of stainless steel weld overlay cladding of reactor pressure vessels subjected to neutron irradiation at a dose of 7.2×10^{19} n cm⁻² (E > 1 MeV) and a flux of 1.1×10^{13} n cm⁻² s⁻¹ at 290 °C were investigated by atom probe tomography and by a nanoindentation technique. To isolate the effects of the neutron irradiation, we compared the results of the measurements of the neutron-irradiated samples with those from a sample aged at 300 °C for a duration equivalent to that of the irradiation. The Cr concentration fluctuation was enhanced in the δ -ferrite phase of the irradiated sample. In addition, enhancement of the concentration fluctuation of Si, which was not observed in the aged sample, was observed. The hardening in the δ -ferrite phase occurred due to both irradiation and aging; however, the hardening of the irradiated sample was more than that expected from the Cr concentration fluctuation, which suggested that the Si concentration fluctuation and irradiation-induced defects were possible origins of the additional hardening.

© 2014 Published by Elsevier B.V.

1. Introduction

Stainless steel weld overlay cladding on the inner surfaces of commercial water-cooled reactor pressure vessels (RPVs) constitutes a protective barrier that protects RPVs from corrosion by cooling water. The cladding material is a duplex phase structure composed of approximately 90% austenite phase and 10% δ -ferrite phase with net-like structures [1]. The mixed δ -ferrite and austenitic phases bring about enhanced corrosion resistance of the cladding [2]. It is known that the δ -ferrite phase is significantly hardened during thermal aging and neutron irradiation, giving rise to an increase in the ductile-to-brittle transition temperature (DBTT) and a decrease in upper-shelf energy [3–8]. However, the relationship between microstructures and the corresponding mechanical properties have not been revealed for neutron-irradiated cladding.

Recently, we investigated the microstructural changes and the hardness in claddings aged at 400 °C for 100–10,000 h by three-dimensional atom probe tomography (APT) [9–11]. Fluctuation in the Cr concentration due to spinodal decomposition was observed, in addition to NiSiMn clusters in the δ -ferrite phase. The hardening

of the δ -ferrite phase with aging showed a good linear relationship with the degree of fluctuation in the Cr concentration, independent of the change in the number and density of the NiSiMn clusters.

We also investigated the microstructural changes in cladding that was neutron-irradiated with a dose of $7.2 \times 10^{19} \, \text{n cm}^{-2}$ ($E > 1 \, \text{MeV}$) and a flux of $1.1 \times 10^{13} \, \text{n cm}^{-2} \, \text{s}^{-1}$ at $290 \, ^{\circ}\text{C}$ by APT [12]. Neutron irradiation resulted in a slight progression in Cr spinodal decomposition and an increase in the fluctuation of the Si, Ni, and Mn concentrations in the δ -ferrite phase. However, the hardness of neutron-irradiated cladding has not been measured.

The objective of this research was to clarify using nanoindentation the contribution of neutron irradiation to the hardness of the cladding and to reveal its origins based on the differences in effects of neutron irradiation and thermal aging on microstructures observed by APT.

2. Experimental

The cladding used was fabricated by an electroslag weld-overlay method, which is same used for actual reactor cladding. The chemical composition is listed in Table 1. The cladding was subjected to post-weld heat treatment (PWHT) at 615 °C for 7 h with subsequent furnace cooling. The sample contained approximately 8% δ -ferrite phase with net-like structures in the matrix

^{*} Corresponding author. Tel.: +81 29 266 7032; fax: +81 29 266 7071. E-mail address: takeuchi.tomoaki@jaea.go.jp (T. Takeuchi).

Table 1 Chemical composition (wt.%) of the sample.

С	Si	Mn	P	S	Ni	Cr	Mo
0.013	0.62	1.28	0.02	0.002	10.7	19.5	0.02

austenite phase. The width of the $\delta\text{-ferrite}$ phase was a few microns. We prepared three samples for experiments by subjecting then to the following treatments: (1) PWHT followed by furnace cooling (as received); (2) neutron irradiation at a dose of $7.2\times10^{19}~n~cm^{-2}~(E>1~MeV)$ and a flux of $1.1\times10^{13}~n~cm^{-2}~s^{-1}$ at 290 °C (with irradiation); and (3) thermal aging at 300 °C for 2000 h (without irradiation), which was equivalent to the temperature (at 290 °C) and time (for 1800 h) during neutron irradiation.

The samples for APT analysis were first lifted using a lift-out method with a dual-beam-focused ion beam scanning electron microscope (FIB/SEM) ion milling system [13], and then they were sharpened to select the austenite or δ -ferrite phase at the tips of the needle-like specimens. To analyze the gallium-free area, the damaged layer caused by gallium implantation during FIB fabrication was minimized by applying low-energy ions during the final process.

A UV laser-pulse APT (CAMECA Instruments LEAP 4000X-HR), equipped with an energy-compensating reflection lens [14–16], was used for the microstructure analysis. The measurements were performed at a laser pulse power of 60 pJ and a repetition rate of 200 kHz at approximately 60 K. The high DC bias was typically in the range of 3–10 kV. A few tens of millions of atoms were typically collected for each measurement.

The samples for nanoindentation were treated by the following procedure as a surface treatment. The samples were mounted in epoxy resin, followed by mechanical polishing with sandpaper and an electrochemical polish in an ethanol solution with a mixture of 5% perchloric acid at 8 °C and finally by a chemical polish in nitro-hydrochloric acid.

Hardness testing was performed using a nanoindenter (ENT-1100a by Elionix Inc.). Because the width of the net-like δ -ferrite phase was only a few microns, as mentioned above, the indentation size needed to be less than a few hundreds nanometers to avoid the influence of the surrounding austenite phase. However, the effect of the surface was likely to appear if the indentation load was overly light. We tried loads of 1, 2, 3, 5, 7, and 9 mN and observed the sizes of the indentations. The SEM image of the indentation at 2 mN is shown in Fig. 1 as an example. With increasing the load, the lowest and mean hardness values tended to shift toward lower values, which likely included the hardness of the

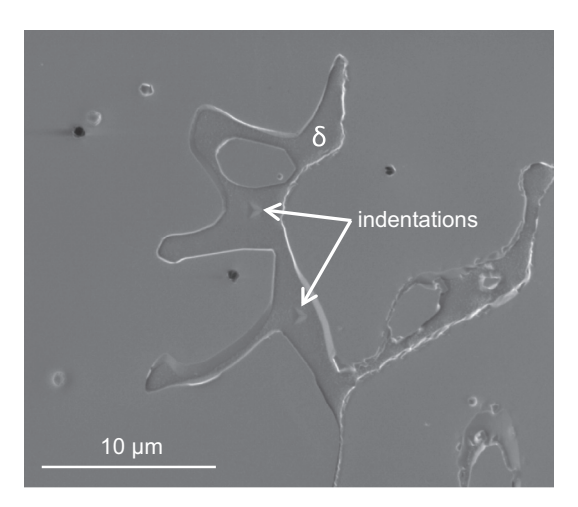


Fig. 1. SEM image of indentations made with loads of 2 mN at the δ -ferrite phase.

austenite phase surrounding the targeted δ -ferrite phase. Therefore, the lower load was as desirable as possible. However, the indentation depth with 1 mN, with which the SEM image of the indentation was no longer clear, was estimated at less than 100 nm where surface effects could exist. As a result, 2 mN was applied in this study as the optimal load, which was the same as that used in Ref. [11]. The average values of hardness were obtained from approximately 10–20 indentations for each sample.

3. Results and discussion

The 3D elemental maps of Fe, Si, Mn, Ni, and Cr in the δ -ferrite phase of the as-received samples, both with and without irradiation, are shown in Fig. 2(a)–(c), respectively. The atom maps are constructed from a slice of 20 nm in thickness to illustrate the detailed chemical composition fluctuations clearly. In Fig. 2, the Cr, Ni, Mn, and Si concentration fluctuations seem to be enhanced after irradiation. However, these fluctuations were too small to be analyzed by a commonly used maximum separation algorithm based on a friend-of-friends concept. Thus, to estimate the concentration fluctuations of Cr, Ni, Si, and Mn, we introduced a parameter V, which is defined as

$$V = \sum_{i=0}^{100} |O(i) - B(i)|, \tag{1}$$

where i is the number of atoms of the element per 100 atoms, and O(i) and B(i) are the observed and binominal distributions of the mean concentration of each element, respectively [17,18]. The distributions should have been similar to a binominal distribution in shape, had the atoms been randomly distributed, resulting in V=0. Fig. 3 shows the correlation between the degrees of the Cr concentration fluctuations ($V_{\rm Cr}$) and $V_{\rm Ni}$, $V_{\rm Si}$, and $V_{\rm Mn}$ for the three samples. $V_{\rm Cr}$ increased with aging without irradiation and increased more with irradiation. In addition, $V_{\rm Ni}$ and $V_{\rm Mn}$ increased while $V_{\rm Si}$ slightly decreased in the sample without irradiation; however, they all increased in the sample with irradiation, compared to the asreceived sample.

Generally, thermal aging enhances the diffusion of mainly oversized atoms because of the vacancy mechanism [19,20]. In contrast, self-interstitial atoms and vacancies are induced by neutron irradiation, resulting in enhancement of the diffusion of undersized and oversized atoms via mixed-dumbbell and vacancy mechanisms, respectively. For the studied samples, the order of the atomic radii was Cr > Mn > (Fe) > Ni > Si [21]. Therefore, the inverse behavior of the V_{Si} value between the irradiated and aged samples was quite reasonable from the viewpoint of the difference in atom sizes [12].

Next, the relationship between the microstructural changes and the hardening at the δ -ferrite phase was studied. The relationship between the V_{Cr} and the nanoindentation hardness in the δ -ferrite phase in the three samples is shown in Fig. 4. A line denoting the results for previously studied thermal-aged samples [11,22,23] was also drawn. The plotted points for the as-received sample and the sample without irradiation were consistent with the correlation line within the margin of error. After irradiation, the point deviated approximately 1 GPa beyond the line outside its margin of error, which implies a cause of hardening other than the Cr concentration fluctuation in the δ -ferrite phase of the sample with irradiation. The fluctuations in Si, Mn, and Ni concentrations and the irradiation-induced defects invisible to APT were possible causes. However, the former is unlikely because the change in Vwas less than 0.1. These trivial concentration fluctuations were considered to hardly affect the motion of dislocations. Therefore, the irradiation-induced defects, such as vacancies and/or their

Download English Version:

https://daneshyari.com/en/article/7967930

Download Persian Version:

https://daneshyari.com/article/7967930

Daneshyari.com